Ionospheric variations following the geomagnetic storm from BeiDou GEO satellite observations: A case study

***Rui Jin*[1, 2], *Shuanggen Jin*[1] *and Xuilin Tao*[3]**

[1] Shanghai Astronomical Observatory, Chinese Academy of Sciences, Shanghai 200030, China, Email: ruijin@shao.ac.cn, sgjin@shao.ac.cn

[2] University of Chinese Academy of Sciences, Beijing 10049, China

[3] Hefei University of Technology, Hefei 230009, China

Abstract

As we known the geomagnetic variation is one of significant factors influencing the Earth's ionosphere. Global Navigation Satellite System (GNSS) has been widely used in studying the ionospheric effect following the geomagnetic storm. However, it is difficult to detect the ionospheric effect during a moderate geomagnetic storm using one GPS observation arc. The BeiDou navigation satellite system (BDS) provides us a new potential means to investigate the ionospheric effect during a moderate geomagnetic storm with its Geostationary Earth Orbit (GEO) satellites' observations. In this paper, the ionospheric behaviors of the geomagnetic storm with the Dst index up to -136 nT during in March 2013 are investigated using the BDS-GEO observations provided by the multi-GNSS experiments (MGEX). Total electron content (TEC) decrease is found following the Strom Sudden Commencements (SSC) and recovers to the normal gradually during the recovery phase of the geomagnetic storm, especially in the South Hemisphere. Furthermore, the ionospheric scintillation enhancement is detected by three BDS stations observations just several hours after the SSC.

1. Introduction

Ionospheric delay error is an important issue for all satellite radio techniques based on electro-magnetic wave signals. As the Earth's ionosphere is a dispersive medium, the phase and amplitude variation of the electro-magnetic wave signals going through the ionosphere will provide an opportunity to sound the Earth's ionosphere. GNSS technique, mainly GPS, has been widely used in Earth's ionospheric monitoring and disturbances detection [1-3]. With more and more constructed GNSS networks, the higher resolution regional or global ionospheric maps with even 4 dimensions can be derived with GNSS dual or multi frequencies measurements [4-6]. The ionospheric model based on GNSS data not only plays an important role in ionospheric delay correction for the electro-magnetic wave propagation, but also monitoring the Earth's ionosphere [7]. What's more, it is also used to study the ionospheric effects of natural disaster, such as pre-seismic ionospheric anomaly and ionospheric disturbance during large geomagnetic storm [2,8]. Currently, the spatial and temporal resolution is still not high enough to monitor the detailed regional ionospheric effects, especially in Asia area, where there are no so many continuously tracking stations except Japan area. The detrend TEC from one arc observations or rate of TEC along the line of sight (LOS) are normally used to study the ionospheric effects and its disturbance patterns following the earthquakes, geomagnetic storms and solar flares [9-10]. Furthermore, it is difficult to distinguish the spatial and temporal variation of the ionosphere using GPS observations due to the satellites' movement.

The GEO satellites of BDS constellation provide us a unique opportunity to monitor the temporal variation and propagation of ionospheric effect following various events that can result in ionospheric anomalies of a fixed area continuously in Earth Centred Earth Fixed coordinate system (ECEF). In this paper, we study the ionospheric behaviours responding to the moderate geomagnetic storms happened on March 17 ,2013 based on BDS observations from the multi-GNSS experiment (MGEX). In Section 2, the BDS observations and TEC retrieval method are introduced. Section 3 shows the ionospheric behaviours following the storm in the areas where the GEO is available. The summary and conclusions are given in Section 4.

2. BDS observations and methods

MGEX is set up by the International GNSS service (IGS) in order to track and analyze all available GNSS signals including GPS, GLONASS, BDS, Galileo, QZSS and space-based augmentation system (SBAS). Up to now, there are about one hundred continuously operating stations all over the world, and thirty of them can track BDS satellites

978-1-4673-5225-3/14/$31.00 ©2014 IEEE

(http://www.igs.org/mgex/network.php). The five GEO satellites of BDS constellation are located in 140° E, 80.3° E, 110° E, 160° E and 58.75° E. As shown in Table 1, three MGEX stations are selected for this study, whose observations have high quality with a relative high satellites elevation, to reduce multipath effect and mapping error.

Table 1 Basic information of the 3 chosen MGEX BDS stations

Station name	Latitude /°	Longitude/°	Height/m	Country
cut0	-32.00	115.50	24.0	Australia
gmsd	30.56	131.02	142.6	Japan
jfng	30.52	114.49	71.3	China

Similar to the GPS, the TEC along the LOS can be expressed with a function of BDS carrier phase or pseudorange measurements as follow:

$$\begin{aligned} TEC &= \frac{f_1^2 f_2^2}{40.28(f_1^2 - f_2^2)}(L_1 - L_2 + \lambda_1 N_1 - \lambda_2 N_2 - c \times DCB) \\ &= \frac{f_1^2 f_2^2}{40.28(f_2^2 - f_1^2)}(P_1 - P_2 - c \times DCB) \end{aligned} \quad (1)$$

where ,*L and P* are the carrier phase and pseudorange measurement, respectively, while the subscript is the frequency number, λ and f are the wavelength and frequency of the signal, *N* is the ambiguity, DCB is the differential code biases and *c* is the light speed in the vacuum. TurboEdit algorithm and time-difference phase ionospheric residual method are used to detect and repair the cycle slips [11-12]. The cosine mapping function is used to convert slant TEC to vertical TEC.

3. Results and discussion

Here the continuous GEO observations at three MGEX stations with the highest satellite elevation angles are used to get the regional TEC variation as shown in the upper three panels in Figure 1. Comparing to the previous quiet days, the TEC at the ionospheric pierce point (IPP) (29.2° S, 115.3° E) decreases dramatically on March 17 and 18, and recovers to the normal condition during the recovery phase. As we known the electron density of the F2 peak can be derived from the critical frequency with the following equation:

$$N_m F_2 = \left(\frac{1}{8.98 \times 10^{-3}} f_0 F_2\right)^2 \quad (2)$$

In generally, the TEC is positively related to the critical frequency. The TEC variation observed by BDS agrees well with the critical frequency's variation detected by the nearby Perth ionosonde station in this period, which is consistent the TEC variation detected by BDS-GEO measurement. However, for the IPP (27.9° N, 114.1° E) and IPP (27.9° N, 132.1° E), the TEC series do not shown obvious anomalous variations. The TEC effect of this storm seems different greatly at different latitudes.

Figure 2 shows the three MGEX stations the standard deviation of the detrended TEC rate (per minute), which can reflect the TEC scintillation in general during the storm from the three BDS-GEO observations. Although they are located in different latitudes and longitudes, the disturbance of the standard deviation is appeared just several hours after the SSC and the amplitude is related to the rate of Dst index. Unlike the TEC series variation, the scintillation in a short period is more likely to the responding to the rate of geomagnetic change during the storm. Although during the recovery phase the Dst index is also relatively lower than the quiet day, but its rate of change is low, so the standard deviation shows no difference in the quiet days.

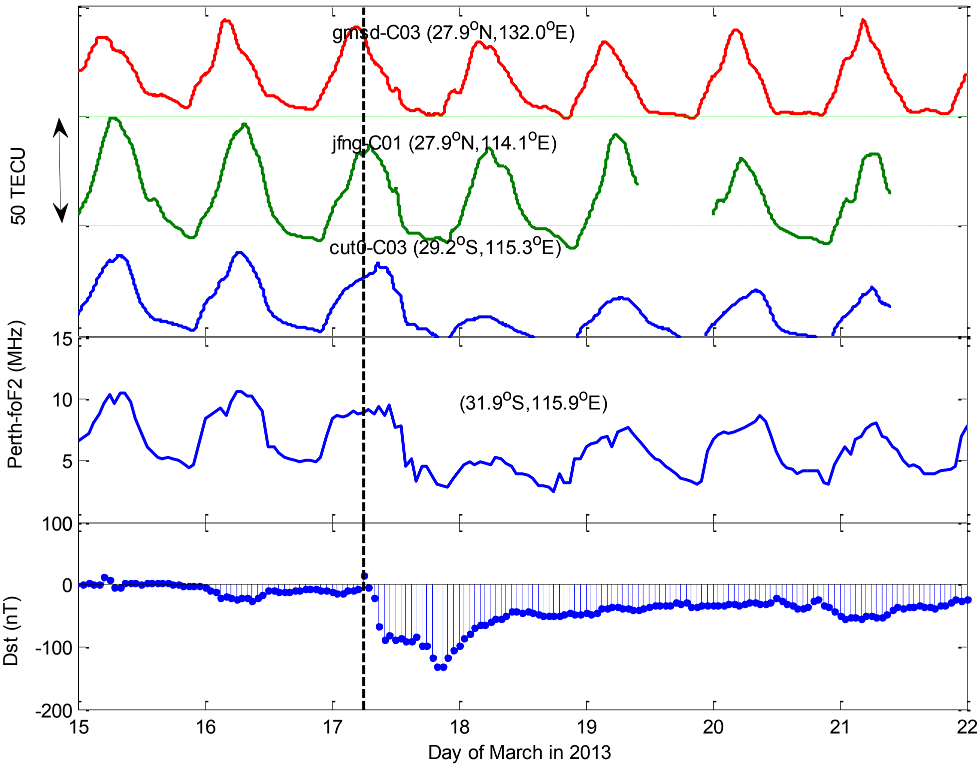

Figure 1. The time series of T EC, f0F2 and Dst during the geomagnetic storm in March 2013. The upper three panels are the TEC variation time series observed by the three MGEX stations, the fourth panel shows the critical frequency variation at Perth from ionosonde (http://spidr.ngdc.noaa.gov), and the bottom panel is the Dst index provided by World Data Center for Geomagnetism, Kyoto (http://wdc.kugi.kyoto-u.ac.jp). The black dash line is the Storm Sudden Commencements (SSC) at UTC 6:00 on March 17).

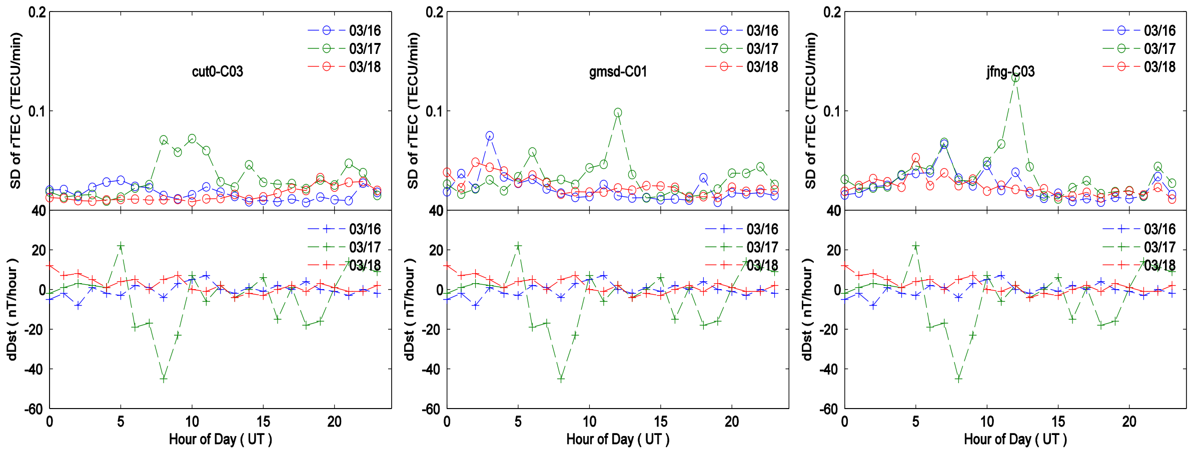

Figure 2. the standard deviation of the detrend TEC rate (per minute). The upper panel presents the hourly standard deviation of the detrended TEC rate (per minute) at three BDS stations (cut0-C03, gmsd-C01, jfng-C03), and the bottom panel shows the hourly variation of Dst index.

respond changing rate? ?

4. Summary and Conclusion

In this paper, we investigated the ionospheric variation during the moderate geomagnetic storm occurred on March 17 in 2013 with BDS-GEO measurement. As the GEO is quasi-invariant in ECEF, we could analyses the TEC temporal variation with a resolution of BDS sampling interval without the effect caused by satellites movement. Using the three MGEX continuously operating stations' GEO measurements at cut0, jfng and gmsd, the TEC decrease is found during the main phase of the storm in the south hemisphere and then recovers to the level of quiet days gradually in the recovery phase. However, the two stations' TEC time series do not show obvious anomaly in the north hemisphere. The TEC variation differs greatly even in the mid-latitudes during this moderate storm. On the other hand, the ionospheric scintillation enhancement is detected by all these three stations just several hours after the SSC. The hourly standard deviation of the detrend TEC rate shows a correlation with the changing rate of the Dst index.

5. Acknowledgments

This research is supported by the Open Research Fund of The Academy of Satellite Application under grant No. 2012-1508, Main Direction Project of Chinese Academy of Sciences (Grant No. KJCX2-EW-T03), Shanghai Science and Technology Commission Project (Grant No. 12DZ2273300) and National Natural Science Foundation of China (NSFC) Project (Grant No. 11173050 and 11373059).

References

1. Hoffmann-Wellenhof B, Lichtenegger H, Collins J. GPS: Theory and practice[J]. 3rd edSpringer-Verlag, New York, 1994.

2. Jin S, Luo O F, Park P. GPS observations of the ionospheric F2-layer behavior during the 20th November 2003 geomagnetic storm over South Korea[J]. Journal of Geodesy, 2008, 82(12): 883-892.

3. Jin, S.G., J. Wang, H. Zhang, and W.Y. Zhu. Real-time monitoring and prediction of the total ionospheric electron content by means of GPS observations, Chin. Astron. Astrophys., 28(3), 331-337, doi: 10.1016/j.chinastron.2004.07.008.

4. Mannucci A J, Wilson B D, Yuan D N, et al. A global mapping technique for GPS‐derived ionospheric total electron content measurements[J]. Radio science, 1998, 33(3): 565-582.

5. Schaer S. Mapping and predicting the Earth's ionosphere using the Global Positioning System[J]. Geod.-Geophys. Arb. Schweiz, Vol. 59,, 1999, 59.

6. Otsuka Y. A new technique for mapping of total electron content using GPS network in Japan[D]. Kyoto University, 2001.

7. Hernández-Pajares M, Juan J M, Sanz J, et al. The IGS VTEC maps: a reliable source of ionospheric information since 1998[J]. Journal of Geodesy, 2009, 83(3-4): 263-275.

8. Liu J Y, Chuo Y J, Shan S J, et al. Pre-earthquake ionospheric anomalies registered by continuous GPS TEC measurements[C]//Annales Geophysicae. 2004, 22(5): 1585-1593.

9. Tsugawa T, Saito A, Otsuka Y, et al. Ionospheric disturbances detected by GPS total electron content observation after the 2011 off the Pacific coast of Tohoku Earthquake[J]. Earth, planets and space, 2011, 63(7): 875-879.

10. Liu J Y, Lin C H, Chen Y I, et al. Solar flare signatures of the ionospheric GPS total electron content[J]. Journal of Geophysical Research: Space Physics (1978–2012), 2006, 111(A5).

11. Blewitt, G. (1990), An Automatic Editing Algorithm for GPS data, Geophys. Res. Lett., 17(3), 199-202.

12. Cai, C., Liu, Z., Xia, P., & Dai, W. (2013). Cycle slip detection and repair for undifferenced GPS observations under high ionospheric activity. GPS solutions, 17(2), 247-260